Fabrication and Optical Synaptic Behavior of MoS_2–WO_3 Heterostructure Memristors: A Comparative Study with Standalone MoS_2 and WO_3 Devices

P HARISH RAGAVENDER
UG3 ECE

Abstract—

In this work, we report the fabrication and characterization of **MoS_2–WO_3 heterostructure-based memristors** and compare their electrical behavior with standalone **MoS_2** and **WO_3** devices. The devices were fabricated using DC sputtering and tested for optical synaptic performance under dark and 450 nm illumination. **MoS_2 standalone exhibited enhanced resistive switching and light-sensitive behavior**, indicating its potential in neuromorphic and optoelectronic applications

Index Terms—MoS_2, WO_3, Heterostructure Memristor, Optical Synapse, Resistive Switching, DC Sputtering, I–V Characterization.

I. Introduction

Two-dimensional (2D) materials such as molybdenum disulfide (MoS_2) and tungsten trioxide (WO_3) have attracted significant attention due to their tunable electronic and optical properties. When combined to form a heterostructure, their synergistic effects can significantly enhance resistive switching and light-sensing behavior. This paper explores the fabrication of MoS_2–WO_3 heterostructure-based memristors and investigates their synaptic switching characteristics under dark and illuminated conditions, in comparison with standalone MoS_2 and WO_3 devices.

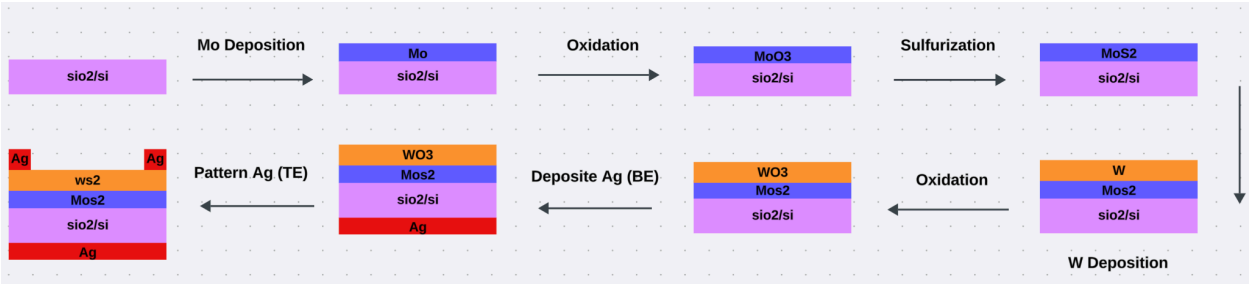

Fig. 1 The device fabrication workflow for MoS_2–WO_3 heterostructure

II. Fabrication Methodology

The device fabrication followed the workflow shown in **Fig. 1**. All layers were deposited using **DC sputtering**. The substrate used was Si/SiO_2.

1. **Mo Layer Deposition:** A Mo layer was deposited on the Si/SiO_2 substrate using DC sputtering.
2. **Oxidation:** The Mo layer was oxidized in ambient air at **550 °C** to form MoO_3.
3. **Sulfurization:** MoO_3 was then sulfurized in a controlled sulfur atmosphere to obtain MoS_2.
4. **W Layer Deposition:** A W layer was sputtered over the MoS_2 layer.
5. **WO_3 Formation:** The W layer was oxidized in ambient air at **550 °C** to form WO_3, resulting in the MoS_2–WO_3 heterostructure.
6. **Electrode Patterning:** Bottom electrodes (Ag) were deposited, Top Ag electrodes were patterned

The same process was followed to fabricate standalone MoS_2 and WO_3 devices

III. Structural and Morphological Analysis

All thin films were deposited using **DC sputtering** under optimized conditions. The oxidation steps were carried out in a tube furnace at **550 °C** in atmospheric conditions for 1 hour to ensure complete formation of oxide layers.

The layer thicknesses were visually confirmed using cross-sectional inspection techniques. Although detailed spectroscopic characterization like Raman or AFM was not performed, the uniformity of deposited films and adhesion was ensured by tuning sputtering power and deposition duration.

IV. Electrical Characterization Setup

All electrical characterizations were carried out using a **Source Measure Unit (SMU)**. I–V characteristics were recorded under the following conditions:

- **Dark:** Room temperature with no external light source.
- **Illuminated:** Exposed to **450 nm LED light** during measurements.

V. Results and Discussion

The resistive switching characteristics of three devices — MoS_2, WO_3, and MoS_2–WO_3 heterostructure — were evaluated using I–V measurements in both dark and 450 nm light illumination. Each condition was analyzed using linear and logarithmic scales to capture subtle switching dynamics and ON/OFF current variations.

A. Linear Scale I–V Characteristics

- **Under Dark:**
  - WO_3 exhibits the lowest current, consistent with its high resistive state.
  - MoS_2 shows higher conduction compared to WO_3 and heterostructure.
  - MoS_2–WO_3 displays intermediate conduction between the two.
- **Under Illumination (450 nm):**
  - WO_3 and MoS_2–WO_3 both show increased photocurrent.
  - **MoS_2 standalone demonstrates the highest photocurrent**, confirming its strong light absorption and efficient carrier modulation.

B. Logarithmic Scale I–V Characteristics

- **Dark (Log scale):**
  - All devices maintain distinguishable low-current states.
  - **MoS_2 exhibits a stronger baseline conductivity** compared to WO_3 and heterostructure devices.
- **Illuminated (Log scale):**
  - All devices show a shift of over one order of magnitude.
  - **MoS_2 standalone exceeds 3 orders of magnitude**, clearly indicating the strongest photo-induced switching behavior.

This comparison demonstrates that **MoS_2 not only improves absolute photocurrent but also significantly enhances resistive switching contrast**, making it highly suitable for optical synaptic applications.

VI. Conclusion

A MoS_2 standalone optical synaptic memristor was successfully fabricated using DC sputtering. Electrical tests under dark and 450 nm light revealed enhanced switching behavior and photo-response in MoS_2 compared to standalone WO_3 and heterostructure devices. The results demonstrate the potential of this simple and scalable fabrication technique for future neuromorphic and optoelectronic applications.

VII. References

[1] L. Hu, J. Yang, J. Wang, P. Cheng, L. O. Chua, and F. Zhuge, “All-Optically Controlled Memristor for Optoelectronic Neuromorphic Computing,” Adv. Funct. Mater., vol. 31, no. 8, p. 2005582, 2021, doi: 10.1002/adfm.202005582.

[2] A. Saleem, D. Kumar, F. Wu, L. B. Keong, and T.-Y. Tseng, “An Opto-Electronic HfOx-Based Transparent Memristive Synapse for Neuromorphic Computing System,” IEEE Trans. Electron Devices, vol. 70, no. 3, pp. 1351–1358, Mar. 2023, doi: 10.1109/TED.2022.3233547.

[3] Y.-X. Hou et al., “Large-Scale and Flexible Optical Synapses for Neuromorphic Computing and Integrated Visible Information Sensing Memory Processing,” ACS Nano, vol. 15, no. 1, pp. 1497–1508, Jan. 2021, doi: 10.1021/acsnano.0c08921.

[4] P. Chen et al., “Recent Progress of 2D Materials for Memristive Devices,” Adv. Funct. Mater., vol. 30, no. 39, p. 2005589, 2020, doi: 10.1002/adfm.202005589.

[5] Z. Wang et al., “Memristors with Diffusive Dynamics as Synaptic Emulators for Neuromorphic Computing,” Nat. Mater., vol. 16, no. 1, pp. 101–108, Jan. 2017, doi: 10.1038/nmat4756.

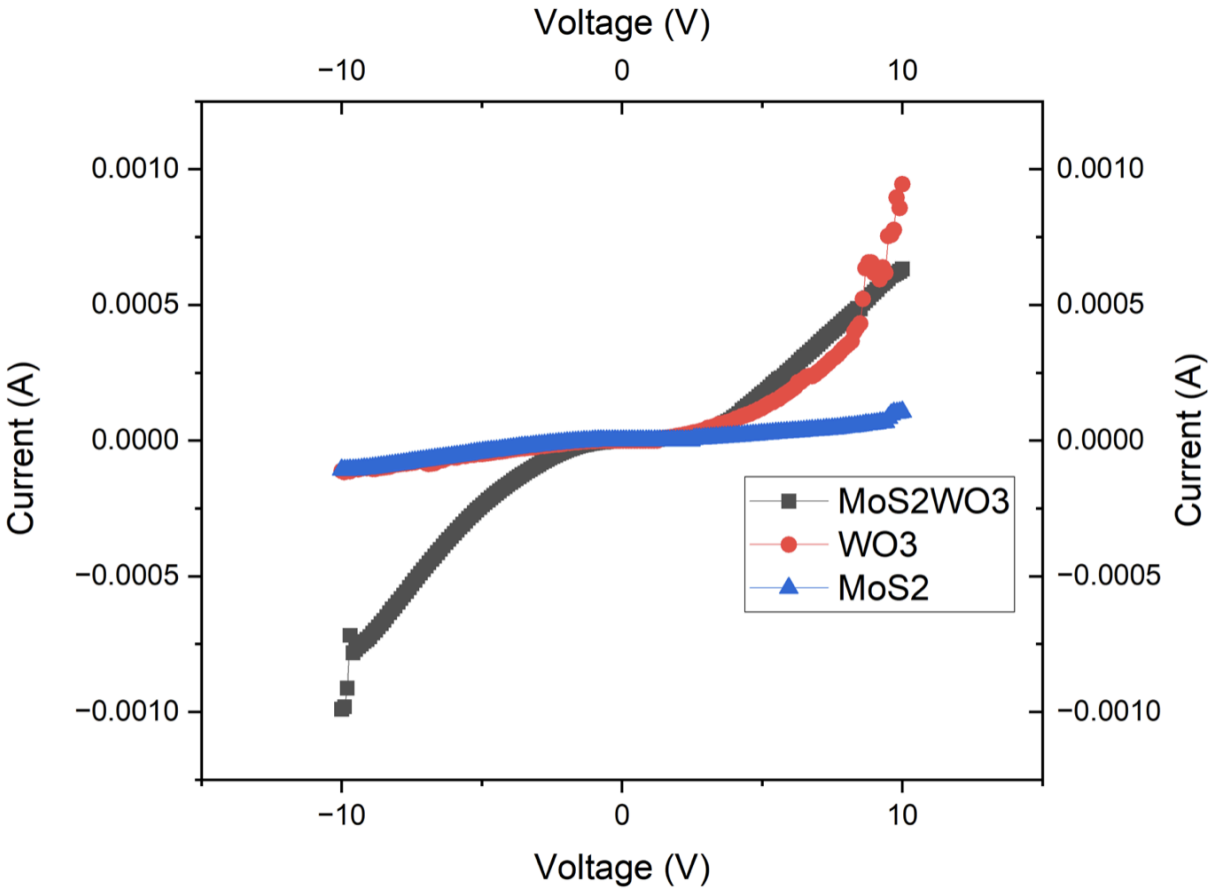

Fig 2a-Dark Condition Linear Scale I–V Characteristics

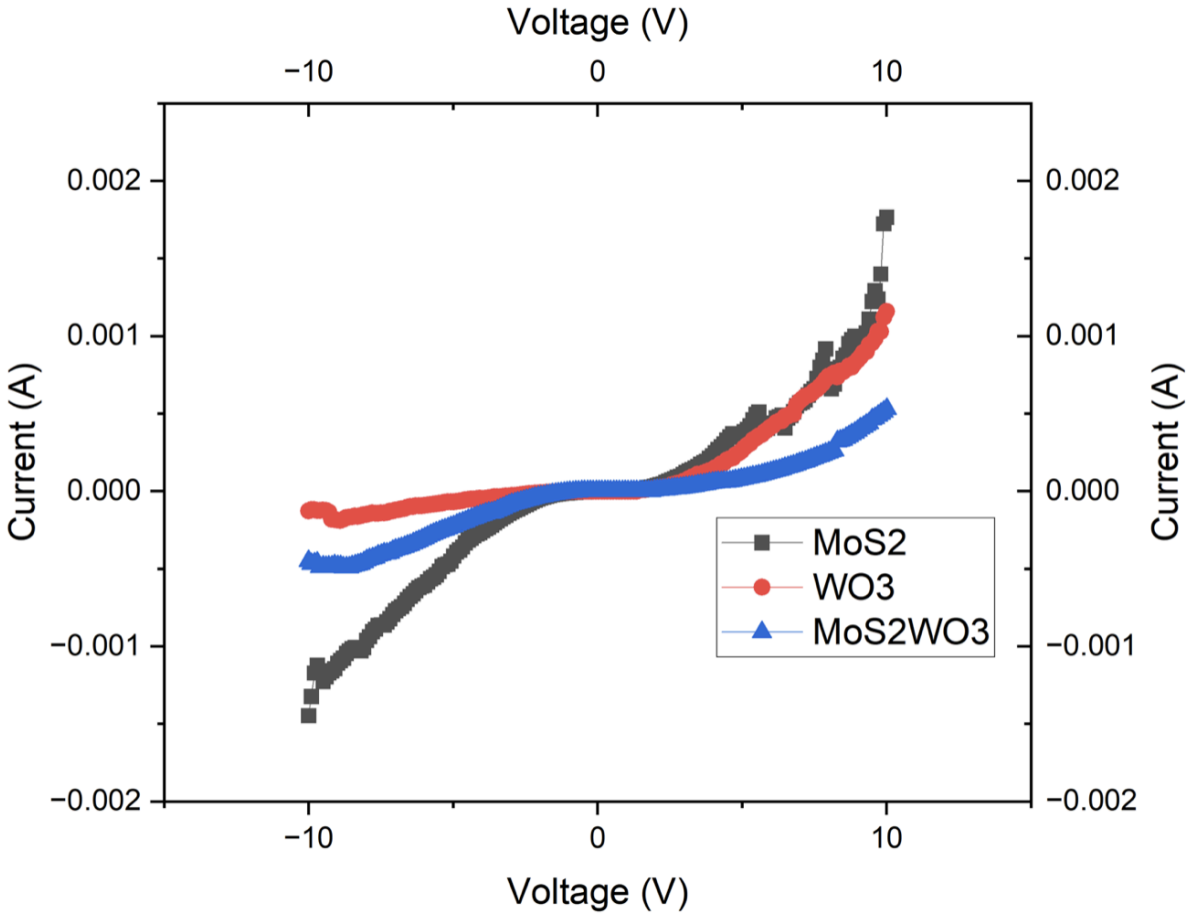

Fig 2b-450 nm illumination Linear Scale I–V Characteristics

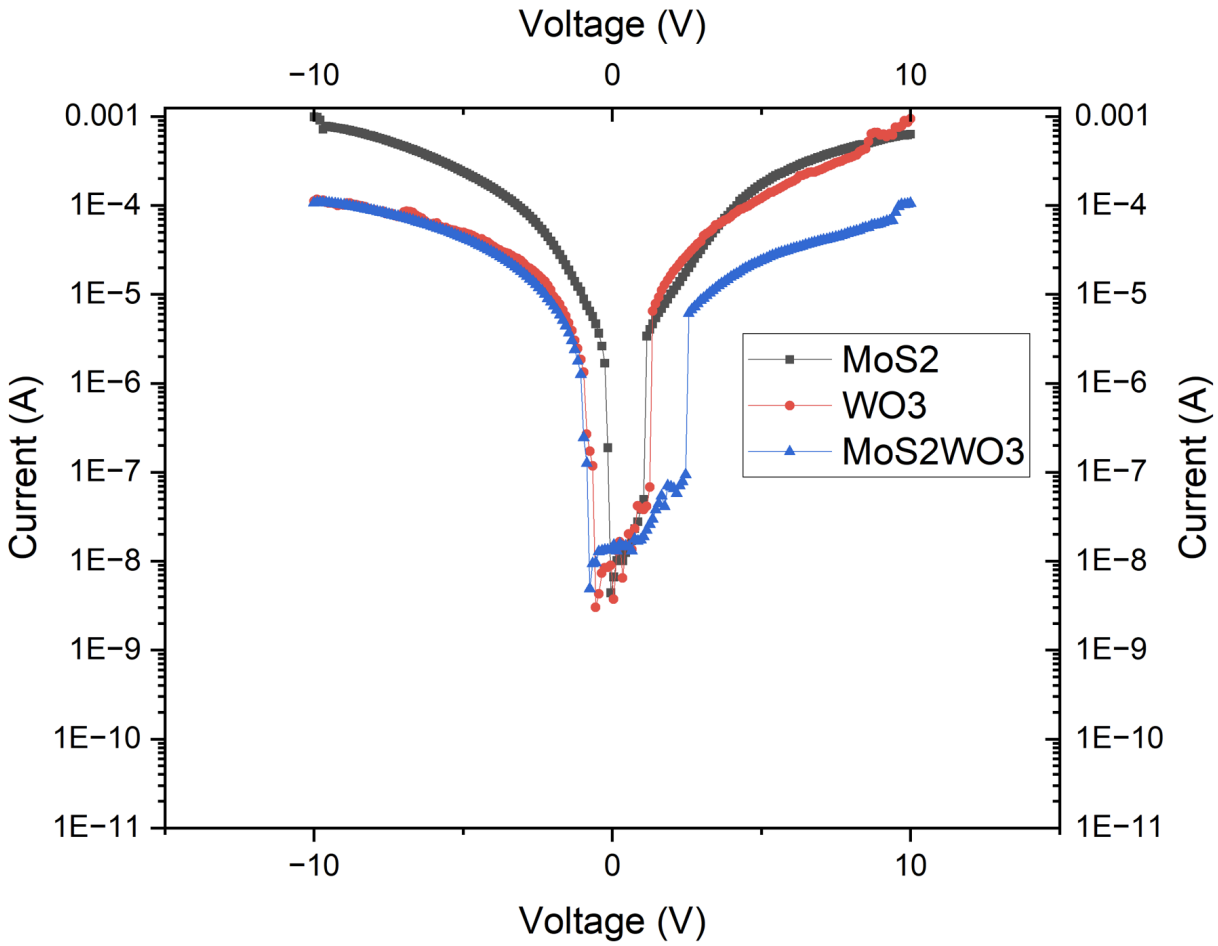

Fig 3a- Dark Condition Log Scale I–V Characteristics

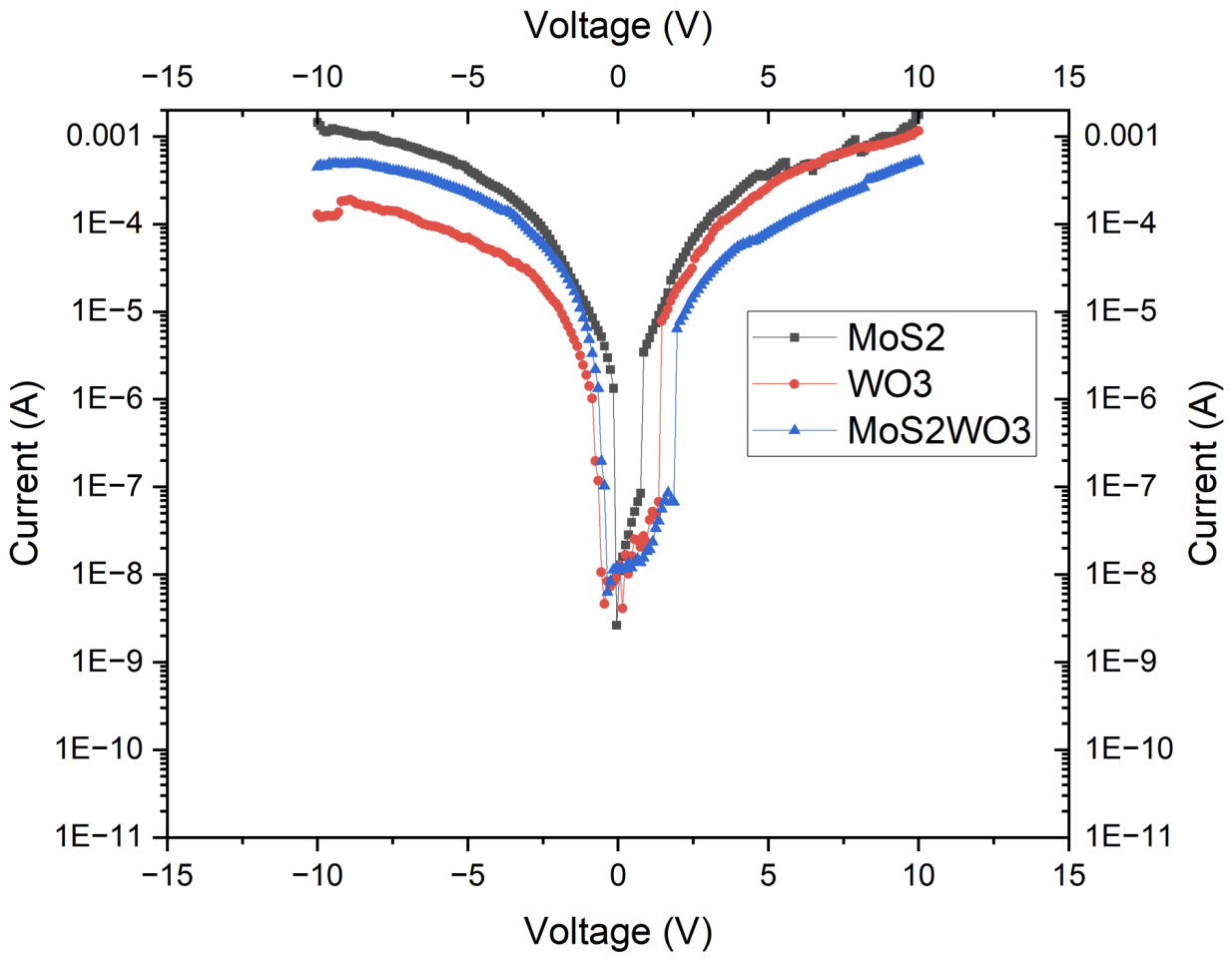

Fig 3b-450 nm illumination Log Scale I–V Characteristics